

# Mononuclear arene ruthenium complexes containing 5,6-diphenyl-3-(pyridine-2-yl)-1,2,4-triazine as chelating ligand: Synthesis and molecular structure

Bruno Therrien\*, Cynthia Saïd-Mohamed, Georg Süss-Fink

*Institut de Chimie, Université de Neuchâtel, Case postale 158, CH-2009 Neuchâtel, Switzerland*

Received 16 May 2007; received in revised form 15 August 2007; accepted 2 November 2007

Available online 7 November 2007

## Abstract

The mononuclear cations of the general formula  $[(\eta^6\text{-arene})\text{RuCl}(\text{pdpt})]^+$  (pdpt = 5,6-diphenyl-3-(pyridine-2-yl)-1,2,4-triazine; arene =  $\text{C}_6\text{H}_6$  (**1**);  $\text{C}_6\text{H}_5\text{Me}$  (**2**); *p*-Pr<sup>i</sup> $\text{C}_6\text{H}_4\text{Me}$  (**3**);  $\text{C}_6\text{Me}_6$  (**4**)) have been synthesised from 5,6-diphenyl-3-(pyridine-2-yl)-1,2,4-triazine (pdpt) and the corresponding chloro complexes  $[(\eta^6\text{-C}_6\text{H}_6)\text{Ru}(\mu\text{-Cl})\text{Cl}]_2$ ,  $[(\eta^6\text{-C}_6\text{H}_5\text{Me})\text{Ru}(\mu\text{-Cl})\text{Cl}]_2$ ,  $[(\eta^6\text{-}i\text{Pr-C}_6\text{H}_4\text{Me})\text{Ru}(\mu\text{-Cl})\text{Cl}]_2$  and  $[(\eta^6\text{-C}_6\text{Me}_6)\text{Ru}(\mu\text{-Cl})\text{Cl}]_2$ , respectively. The X-ray crystal structure analyses of  $[\mathbf{1}][\text{PF}_6] \cdot (\text{C}_6\text{H}_6)_{2.5}$  and  $[\mathbf{2}][\text{PF}_6] \cdot (\text{CH}_3\text{CN})_2$  reveal a typical piano-stool geometry around the metal centre and in the crystal packing a complexed networks of intermolecular interactions.

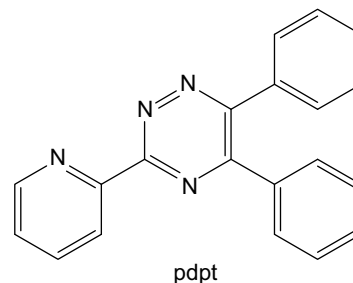
© 2007 Elsevier B.V. All rights reserved.

**Keywords:** Arene ligands; N ligand; Polypyridyl ligand; Ruthenium

## 1. Introduction

Ruthenium complexes attract more and more attention in view of their applications as biological active species [1]. Two ruthenium-based anticancer drugs, NAMI-A [2] and KP1019 [3], have completed phase I clinical trials and are scheduled to enter phase II in the near future (see Fig. 1). Among classical ruthenium anticancer drugs, polypyridyl–Ru systems have been used as molecular DNA probes owing to their photoluminescence properties and ability to intercalate DNA [4]. These potential DNA-targeting anticancer agents have been screened for anticancer activity. Numerous examples of polypyridyl–Ru complexes including [2,2′-bipyridine, 1,10-phenanthroline, 2,2′:6′2′-terpyridine] have been studied [5]. In all cases, their biological activity was related to their ability to intercalate DNA.

Similarly, organometallic  $\eta^6$ -arene ruthenium complexes have been investigated as anticancer drug candidates. They are known to interact with DNA to form monofunctional DNA adducts [4c,6]. Therefore, we were interested in combining an arene ruthenium moiety with a polypyridyl ligand able to interact with DNA at its periphery. Herein we report on the synthesis and characterisation of mononuclear arene ruthenium complexes with the polypyridyl chelate ligand, 5,6-diphenyl-3-(pyridine-2-yl)-1,2,4-triazine (pdpt). After coordination to the ruthenium atom, the pdpt ligand still possesses a free pyridyl function for intermolecular interactions.



\* Corresponding author. Tel.: +41 032 7182499; fax: +41 032 7182511.  
E-mail address: bruno.therrien@unine.ch (B. Therrien).

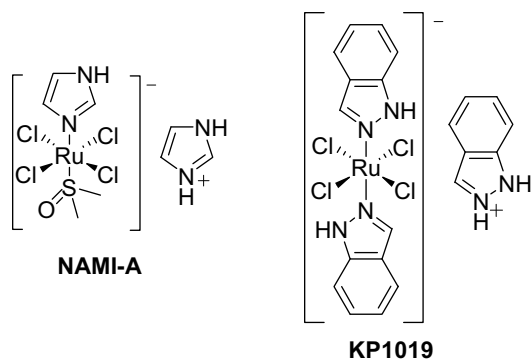


Fig. 1. Clinically evaluated ruthenium-based anticancer drugs.

## 2. Experimental

### 2.1. General remarks

5,6-Diphenyl-3-(pyridine-2-yl)-1,2,4-triazine (pdpt) and  $\text{KPF}_6$  were purchased from Aldrich and used as received.  $[(\eta^6\text{-arene})\text{Ru}(\mu\text{-Cl})\text{Cl}]_2$  (arene =  $\text{C}_6\text{H}_6$ ,  $\text{C}_6\text{H}_5\text{Me}$ ,  $p\text{-Pr}^i\text{C}_6\text{H}_4\text{Me}$ ,  $\text{C}_6\text{Me}_6$ ) were prepared according to the published methods [7]. The NMR spectra were recorded on a Bruker AMX 400 MHz spectrometer using the residual protonated solvent as internal standard. Infrared spectra were recorded as KBr pellets on a Perkin–Elmer FTIR 1720-X spectrometer. UV–Vis absorption spectra were recorded on an Uvikon 930 spectrophotometer. Microanalyses were performed by the Laboratory of Pharmaceutical Chemistry, University of Geneva (Switzerland). Electro-spray mass spectra were obtained in positive-ion mode with an LCQ Finnigan mass spectrometer.

### 2.2. $[(\eta^6\text{-C}_6\text{H}_6)\text{RuCl}(\text{pdpt})][\text{PF}_6]$ (**[1]** $[\text{PF}_6]$ )

$[(\eta^6\text{-C}_6\text{H}_6)\text{Ru}(\mu\text{-Cl})\text{Cl}]_2$  (100 mg, 0.20 mmol), pdpt (124 mg, 0.40 mmol) and  $\text{KPF}_6$  (73.6 mg, 0.40 mmol) are dissolved in methanol (30 mL). The mixture is heated to 50 °C and stirred for 4 h. After cooling to room temperature, the volume is reduced and the product is precipitated by the addition of diethylether. The orange solid is filtered, washed with *n*-pentane and dried under vacuum to give  $[(\eta^6\text{-C}_6\text{H}_6)\text{RuCl}(\text{pdpt})][\text{PF}_6]$  (60 mg, 0.09 mmol, yield 22%).  $^1\text{H}$  NMR (400 MHz,  $\text{CD}_3\text{CN}$ ):  $\delta$  (ppm) = 6.14 (s, 6H,  $\text{C}_6\text{H}_6$ ), 7.53 (m, 4H,  $\text{C}_6\text{H}_5$ ), 7.63 (m, 2H,  $\text{C}_6\text{H}_5$ ), 7.75 (m, 4H,  $\text{C}_6\text{H}_5$ ), 7.89 (dd, 1H,  $^3J = 5.6$  Hz,  $\text{C}_5\text{H}_4\text{N}$ ), 8.31 (dd, 1H,  $^3J = 7.8$  Hz,  $\text{C}_5\text{H}_4\text{N}$ ), 8.68 (d, 1H,  $^3J = 10$  Hz,  $\text{C}_5\text{H}_4\text{N}$ ), 9.52 (d, 1H,  $^3J = 7.6$  Hz,  $\text{C}_5\text{H}_4\text{N}$ ); IR (KBr,  $\text{cm}^{-1}$ ):  $\nu(\text{P-F})$  840s; 558m. UV–Vis ( $6.6 \times 10^{-5}$  M,  $\text{CH}_3\text{CN}$ ):  $\lambda_{\text{max}}$  298 nm ( $\epsilon = 0.97 \times 10^4 \text{ M}^{-1} \text{ cm}^{-1}$ ); ESI-MS ( $m/z$ ): 525  $[\text{M}^+]$ ; Anal. Calc. for  $\text{C}_{26}\text{H}_{20}\text{N}_4\text{ClF}_6\text{PRu}$ : C, 46.61; H, 3.01; N, 8.36. Found: C, 46.60; H, 3.61; N, 8.05%.

### 2.3. $[(\eta^6\text{-C}_6\text{H}_5\text{Me})\text{RuCl}(\text{pdpt})][\text{PF}_6]$ (**[2]** $[\text{PF}_6]$ )

$[(\eta^6\text{-C}_6\text{H}_5\text{Me})\text{Ru}(\mu\text{-Cl})\text{Cl}]_2$  (100 mg, 0.19 mmol), pdpt (117.5 mg, 0.38 mmol) and  $\text{KPF}_6$  (69.7 mg, 0.38 mmol)

are dissolved in methanol (30 mL). The mixture is heated to 50 °C and stirred for 4 h. After cooling to room temperature, the volume is reduced and the product is precipitated by the addition of diethylether. The orange–brown solid is filtered, washed with *n*-pentane and dried under vacuum to give  $[(\eta^6\text{-C}_6\text{H}_5\text{Me})\text{RuCl}(\text{pdpt})][\text{PF}_6]$  (170 mg, 0.25 mmol, yield 66%).  $^1\text{H}$  NMR (400 MHz,  $\text{CD}_3\text{CN}$ ):  $\delta$  (ppm) = 2.34 (s, 3H,  $\text{C}_6\text{H}_5\text{CH}_3$ ), 5.79 (d, 1H,  $^3J = 6.0$  Hz,  $\text{C}_6\text{H}_5\text{CH}_3$ ), 5.83 (d, 1H,  $\text{C}_6\text{H}_5\text{CH}_3$ ), 5.85 (dd, 1H,  $^3J = 5.9$  Hz,  $\text{C}_6\text{H}_5\text{CH}_3$ ), 6.13 (dd, 1H,  $\text{C}_6\text{H}_5\text{CH}_3$ ), 6.18 (dd, 1H,  $\text{C}_6\text{H}_5\text{CH}_3$ ), 7.46 (m, 6H,  $\text{C}_6\text{H}_5$ ), 7.72 (m, 4H,  $\text{C}_6\text{H}_5$ ), 7.88 (dd, 1H,  $^3J = 5.6$  Hz,  $\text{C}_5\text{H}_4\text{N}$ ), 8.30 (dd, 1H,  $^3J = 7.8$  Hz,  $\text{C}_5\text{H}_4\text{N}$ ), 8.68 (d, 1H,  $^3J = 9.4$  Hz,  $\text{C}_5\text{H}_4\text{N}$ ), 9.45 (d, 1H,  $^3J = 7.6$  Hz,  $\text{C}_5\text{H}_4\text{N}$ ); IR (KBr,  $\text{cm}^{-1}$ ):  $\nu(\text{P-F})$  838s; 558m; UV–Vis ( $5.9 \times 10^{-6}$  M,  $\text{CH}_3\text{CN}$ ):  $\lambda_{\text{max}}$  298 nm ( $\epsilon = 9.76 \times 10^4 \text{ M}^{-1} \text{ cm}^{-1}$ ); ESI-MS ( $m/z$ ): 539  $[\text{M}^+]$ ; Anal. Calc. for  $\text{C}_{27}\text{H}_{22}\text{N}_4\text{ClF}_6\text{PRu}$ : C, 47.41; H, 3.24; N, 8.19. Found: C, 47.19; H, 3.37; N, 8.37%.

### 2.4. $[(\eta^6\text{-}p\text{-Pr}^i\text{C}_6\text{H}_4\text{Me})\text{RuCl}(\text{pdpt})][\text{PF}_6]$ (**[3]** $[\text{PF}_6]$ )

$[(\eta^6\text{-}p\text{-Pr}^i\text{C}_6\text{H}_4\text{Me})\text{Ru}(\mu\text{-Cl})\text{Cl}]_2$  (100 mg, 0.16 mmol),  $\text{C}_{20}\text{H}_{14}\text{N}_4$  (101.34 mg, 0.32 mmol) and  $\text{KPF}_6$  (60.15 mg, 0.32 mmol) are dissolved in methanol (30 mL). The mixture is heated to 50 °C and stirred for 4 h. After cooling to room temperature, the volume is reduced and the product is precipitated by the addition of diethylether. The brown solid is filtered, washed with *n*-pentane and dried under vacuum to give  $[(\eta^6\text{-}p\text{-Pr}^i\text{C}_6\text{H}_4\text{Me})\text{RuCl}(\text{pdpt})][\text{PF}_6]$  (120 mg, 0.16 mmol, yield 51%).  $^1\text{H}$  NMR (400 MHz,  $\text{CD}_3\text{CN}$ ):  $\delta$  (ppm) = 1.20 (d, 3H,  $^3J = 3.4$  Hz,  $\text{CH}(\text{CH}_3)_2$ ), 1.22 (d, 3H,  $^3J = 3.5$  Hz,  $\text{CH}(\text{CH}_3)_2$ ), 2.17 (s, 3H,  $\text{CH}_3$ ), 2.89 (sept, 1H,  $^3J = 6.9$  Hz,  $\text{CH}(\text{CH}_3)_2$ ), 5.80 (d, 1H,  $^3J = 6.2$  Hz,  $\text{C}_6\text{H}_4$ ), 5.85 (d, 1H,  $^3J = 6.3$  Hz,  $\text{C}_6\text{H}_4$ ), 6.01 (d, 1H,  $\text{C}_6\text{H}_4$ ), 6.03 (d, 1H,  $\text{C}_6\text{H}_4$ ), 7.52 (dd, 2H,  $\text{C}_6\text{H}_5$ ), 7.55 (dd, 2H,  $\text{C}_6\text{H}_5$ ), 7.65 (m, 2H,  $\text{C}_6\text{H}_5$ ), 7.75 (m, 4H,  $\text{C}_6\text{H}_5$ ), 7.91 (dd, 1H,  $^3J = 5.6$  Hz,  $\text{C}_5\text{H}_4\text{N}$ ), 8.31 (dd, 1H,  $^3J = 7.9$  Hz,  $\text{C}_5\text{H}_4\text{N}$ ), 8.69 (d, 1H,  $^3J = 10$  Hz,  $\text{C}_5\text{H}_4\text{N}$ ), 9.44 (d, 1H,  $^3J = 7.5$  Hz,  $\text{C}_5\text{H}_4\text{N}$ ); IR (KBr,  $\text{cm}^{-1}$ ):  $\nu(\text{P-F})$  839s; 558m; UV–Vis ( $1.0 \times 10^{-5}$  M,  $\text{CH}_3\text{CN}$ ):  $\lambda_{\text{max}}$  300 nm ( $\epsilon = 3.29 \times 10^4 \text{ M}^{-1} \text{ cm}^{-1}$ ); ESI-MS ( $m/z$ ): 581  $[\text{M}^+]$ ; Anal. Calc. for  $\text{C}_{30}\text{H}_{28}\text{N}_4\text{ClF}_6\text{PRu}$ : C, 49.63; H, 3.89; N, 7.72. Found: C, 49.19; H, 3.91; N, 7.69%.

### 2.5. $[(\eta^6\text{-C}_6\text{Me}_6)\text{RuCl}(\text{pdpt})][\text{PF}_6]$ (**[4]** $[\text{PF}_6]$ )

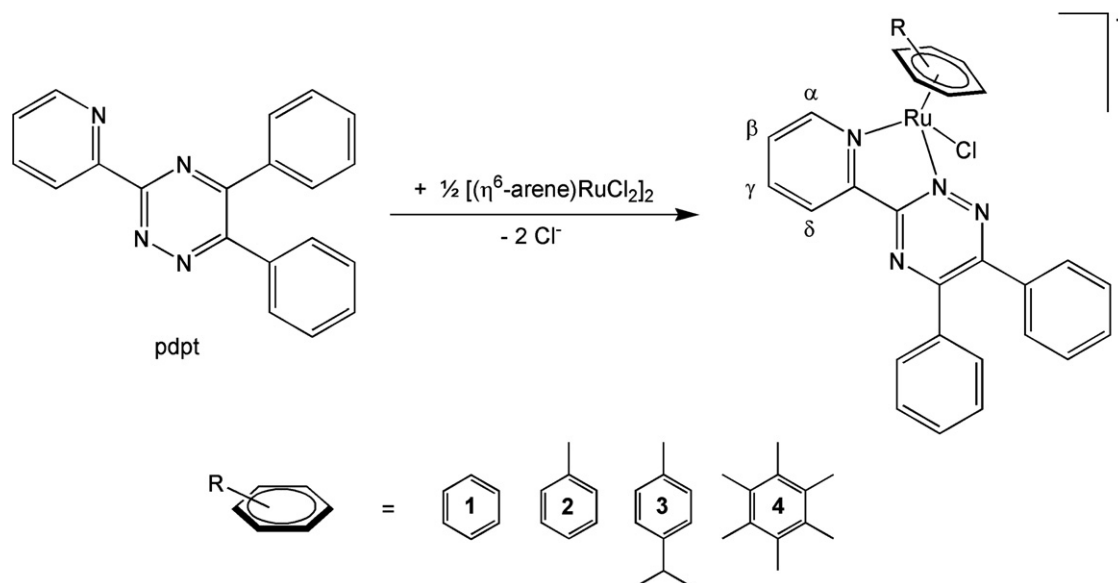
$[(\eta^6\text{-C}_6\text{Me}_6)\text{Ru}(\mu\text{-Cl})\text{Cl}]_2$  (100 mg, 0.15 mmol),  $\text{C}_{20}\text{H}_{14}\text{N}_4$  (92.8 mg, 0.30 mmol) and  $\text{KPF}_6$  (55.10 mg, 0.30 mmol) are dissolved in methanol (30 mL). The mixture is heated to 50 °C and stirred for 4 h. After cooling to room temperature, the volume is reduced and the product is precipitated by the addition of diethylether. The dark red solid is filtered, washed with *n*-pentane and dried under vacuum to give  $[(\eta^6\text{-C}_6\text{Me}_6)\text{RuCl}(\text{pdpt})][\text{PF}_6]$  (120 mg, 0.16 mmol, yield 53%).  $^1\text{H}$  NMR (400 MHz,  $\text{CD}_3\text{CN}$ ):  $\delta$  (ppm) = 2.19 (s, 18H,  $\text{C}_6(\text{CH}_3)_6$ ), 7.44 (dd, 2H,  $^3J = 7.9$  Hz,  $\text{C}_6\text{H}_5$ ), 7.54 (m, 6H,  $\text{C}_6\text{H}_5$ ), 7.73 (d, 2H,

Table 1  
Crystallographic and selected experimental data for  $[1][PF_6] \cdot (C_6H_6)_{2.5}$   
and  $[2][PF_6] \cdot (CH_3CN)_2$

	$[1][PF_6] \cdot (C_6H_6)_{2.5}$	$[2][PF_6] \cdot (CH_3CN)_2$
Chemical formula	$C_{41}H_{35}ClF_6N_4PRu$	$C_{31}H_{28}ClF_6N_6PRu$
Formula weight	865.22	766.08
Crystal system	monoclinic	monoclinic
Space group	$P2_1/n$ (No. 14)	$P2_1/n$ (No. 14)
Crystal colour and shape	red block	red needle
Crystal size	$0.18 \times 0.14 \times 0.13$	$0.32 \times 0.08 \times 0.07$
$a$ (Å)	15.716(1)	8.5006(5)
$b$ (Å)	10.8734(6)	20.086(2)
$c$ (Å)	22.995(2)	18.890(1)
$\beta$ (°)	98.695(6)	124.652(6)
$V$ (Å <sup>3</sup> )	3884.3(5)	3199.1(4)
$Z$	4	4
$T$ (K)	173(2)	173(2)
$D_{calc}$ (g cm <sup>-3</sup> )	1.480	1.591
$\mu$ (mm <sup>-1</sup> )	0.578	0.691
Scan range (°)	$1.70 < \theta < 25.66$	$1.49 < \theta < 25.66$
Unique reflections	7311	5585
Observed reflections	4805	3836
$[I > 2\sigma(I)]$		
$R_{int}$	0.0730	0.2008
Final $R$ indices $[I > 2\sigma(I)]^a$	0.0433, $wR_2$ 0.0944	0.1196, $wR_2$ 0.3046
$R$ indices (all data)	0.0774, $wR_2$ 0.1022	0.1547, $wR_2$ 0.3202
Goodness-of-fit	0.903	1.144
Maximum, minimum $\Delta\rho/e$ (Å <sup>-3</sup> )	0.877, -0.601	2.296, -2.387

<sup>a</sup> Structure was refined on  $F_o^2$ :  $wR_2 = [\sum[w(F_o^2 - F_c^2)^2] / \sum w(F_o^2)^2]^{1/2}$ , where  $w^{-1} = [\sum(F_o^2) + (aP)^2 + bP]$  and  $P = [\max(F_o^2, 0) + 2F_c^2]/3$ .

$C_6H_5$ ), 7.93 (dd, 1H,  $^3J = 5.6$  Hz,  $C_5H_4N$ ), 8.26 (dd, 1H,  $^3J = 7.8$  Hz,  $C_5H_4N$ ), 8.68 (d, 1H,  $^3J = 10$  Hz,  $C_5H_4N$ ), 9.03 (d, 1H,  $^3J = 7.6$  Hz,  $C_5H_4N$ ); IR (KBr, cm<sup>-1</sup>):  $\nu$ (P-F) 840s; 558m; UV-Vis ( $1.1 \times 10^{-5}$  M,  $CH_3CN$ ):  $\lambda_{max}$  439 nm ( $\epsilon = 0.45 \times 10^4$  M<sup>-1</sup> cm<sup>-1</sup>), 295 nm ( $\epsilon = 1.63 \times 10^4$  M<sup>-1</sup> cm<sup>-1</sup>); ESI-MS ( $m/z$ ): 609 [ $M^+$ ]; Anal. Calc. for  $C_{32}H_{32}N_4ClF_6PRu$ : C, 50.97; H, 4.28; N, 7.43. Found: C, 50.71; H, 4.40; N, 7.47%.



Scheme 1. Synthesis of cations 1–4.

## 2.6. X-ray crystallographic study

Crystals of  $[1][PF_6] \cdot (C_6H_6)_{2.5}$  are obtained by the slow evaporation of a chloroform/benzene solution of  $[1][PF_6]$ , while the crystals of  $[2][PF_6] \cdot (CH_3CN)_2$  are obtained by the slow evaporation of an acetonitrile solution of  $[2][PF_6]$ . The data were measured using a Bruker SMART CCD diffractometer, using Mo  $K\alpha$  graphite monochromated radiation ( $\lambda = 0.71073$  Å). The structures were solved by direct methods using the program SHELXS-97 [8]. The refinement and all further calculations were carried out using SHELXL-97 [8]. The H-atoms were included in calculated positions and treated as riding atoms using the SHELXL default parameters. The non-H atoms were refined anisotropically, using weighted full-matrix least-square on  $F^2$ . Crystallographic details are summarised in Table 1. Figs. 3 and 4 are drawn with ORTEP [9] and Figs. 5–7 with MERCURY [10].

## 3. Results and discussion

The arene ruthenium complexes  $[(\eta^6\text{-arene})Ru(\mu\text{-Cl})Cl]_2$  (arene =  $C_6H_6$ ,  $C_6H_5Me$ ,  $p\text{-Pr}^iC_6H_4Me$ ,  $C_6Me_6$ ) react with two equivalents of 5,6-diphenyl-3-(pyridine-2-yl)-1,2,4-triazine (pdpt) in methanol at 50 °C in the presence of  $KPF_6$  to form the cationic arene ruthenium complexes  $[(\eta^6\text{-}C_6H_6)RuCl(pdpt)]^+$  (1),  $[(\eta^6\text{-}C_6H_5Me)RuCl(pdpt)]^+$  (2),  $[(\eta^6\text{-}p\text{-Pr}^iC_6H_4Me)RuCl(pdpt)]^+$  (3) and  $[(\eta^6\text{-}C_6Me_6)RuCl(pdpt)]^+$  (4), which are isolated as their hexafluorophosphate salts (Scheme 1). The hexafluorophosphate salts of complexes 1–4 are orange–brown, non-hygroscopic, air-stable solids. They are sparingly soluble in methanol, chloroform and water, but well soluble in dichloromethane, acetone and acetonitrile. All compounds have been characterised on the basis of elemental analysis, <sup>1</sup>H NMR, IR, UV–Vis and mass spectroscopy.

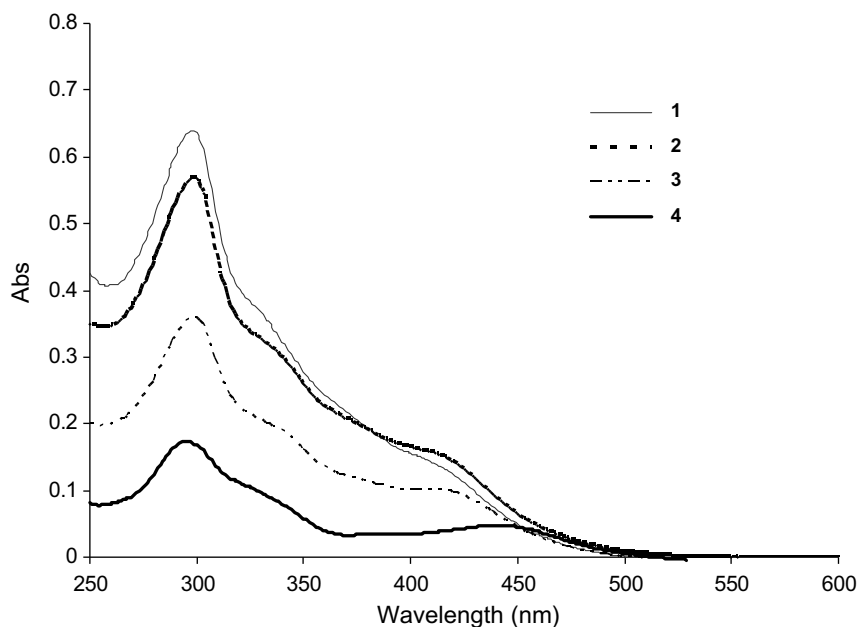


Fig. 2. UV-Vis absorption data of 1–4 in acetonitrile at 298 K.

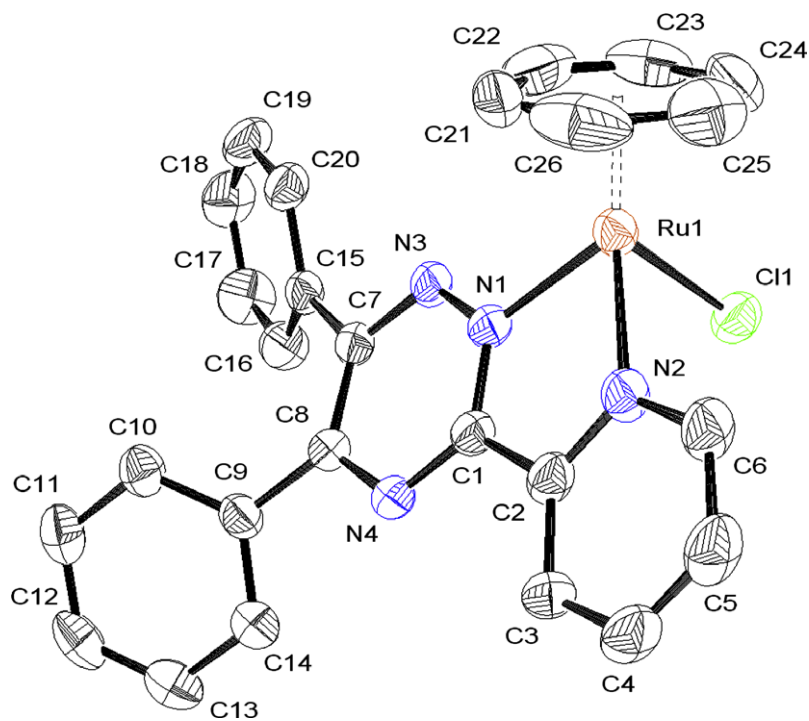


Fig. 3. Molecular structure of 1 at 50% probability level with hydrogen atoms, benzene molecules and hexafluorophosphate anion have been omitted for clarity.

In the mass spectra they give rise to the corresponding  $[M]^+$  molecular peaks  $m/z$  at 525, 539, 581 and 609, respectively. The  $^1\text{H}$  NMR spectra of 1–4 exhibit, other than the signals corresponding to the  $\eta^6$ -aromatic ligand, a characteristic set of fourteen signals for the diastereotopic protons of the pdpt ligand. The ruthenium atom is stereogenic due to the coordination of four different ligand atoms. Upon coordination to the ruthenium atom, the aromatic protons

of the pdpt ligand are shifted downfield, especially the  $\text{H}_\alpha$  of the coordinated pyridyl group which is observed at  $\delta > 9.0$  ppm, while the  $\text{H}_\beta$  is observed at only 8.7 ppm. Accordingly, the aromatic protons of the phenyl groups are observed as multiplet at  $\delta \sim 7.45$  and 7.75 ppm. The  $^1\text{H}$  NMR spectrum of 3 exhibits two doublets for the diastereotopic methyl protons of the isopropyl group. Likewise, the diastereotopic CH protons of the *p*-cymene

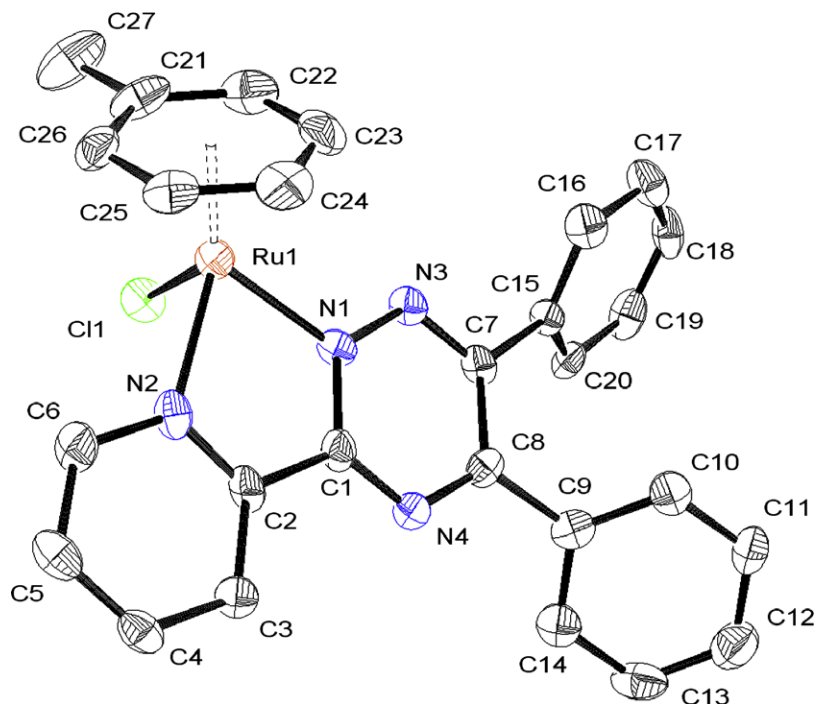


Fig. 4. Molecular structure of **2** at 50% probability level with hydrogen atoms, acetonitrile molecules and hexafluorophosphate anion have been omitted for clarity.

ligand give rise to four doublets observed between  $\delta = 5.8$ – $6.1$  ppm. A septet at  $\delta = 2.89$  ppm is observed for the CH proton of the isopropyl group. Similarly, the aromatic protons of the toluene ligand in **2** give rise to five multiplets observed between  $\delta = 5.79$ – $6.18$  ppm and a singlet at  $\delta = 2.17$  ppm for the methyl group.

The UV–Vis data of complexes **1–4** have been recorded in acetonitrile, see Fig. 2. The electronic spectra display a low energy absorption band in the visible region at  $\sim 440$  nm and an intense band at  $\sim 300$  nm. The low intensity band at  $\sim 440$  nm is assigned to the metal-to-ligand charge transfer transition (MLCT), while the high-energy band at  $\sim 300$  nm is assigned to intra-ligand  $\pi$ – $\pi^*$  transitions [11].

The molecular structures of  $[(\eta^6\text{-C}_6\text{H}_6)\text{RuCl}(\text{pdpt})]^+$  (**1**) and  $[(\eta^6\text{-C}_6\text{H}_5\text{Me})\text{RuCl}(\text{pdpt})]^+$  (**2**) have been established by single-crystal X-ray structure analysis of their hexafluorophosphate salts. The complexes show typical piano-stool geometry with the metal centre coordinated by the arene ligand, a terminal chloride and the chelating pdpt ligand. The molecular structures of **1** and **2** are shown in Figs. 3 and 4, respectively, and a series of selected geometrical parameters are presented in Table 2.

In the mononuclear complexes **1** and **2**, the metal centres are stereogenic. However, since none of the ligands contains chiral information, they are both obtained as a racemic mixture and crystallised in the centrosymmetric space group  $P2_1/n$ . The Ru–N bond distances 2.05 and 2.09 Å in **1** and **2** are comparable to those in  $[(\eta^6\text{-}p\text{-Pr}^i\text{C}_6\text{H}_4\text{Me})\text{RuCl}(2,3\text{-bis}(2\text{-pyridyl})\text{pyrazine})][\text{BF}_4]$  [12],  $[(\eta^6\text{-}p\text{-Pr}^i\text{C}_6\text{H}_4$

$\text{Me})\text{RuCl}(2,3\text{-bis}(\alpha\text{-pyridyl})\text{quinoxaline})][\text{PF}_6]$  [13],  $[(\eta^6\text{-C}_6\text{H}_6)\text{RuCl}(\text{dpqMe}_2)][\text{PF}_6]$  ( $\text{dpqMe}_2 = 6,7\text{-dimethyl-2,3-di}(\text{pyridine-2-yl})\text{quinoxaline}$ ) and  $[(\eta^6\text{-}p\text{-Pr}^i\text{C}_6\text{H}_4\text{Me})\text{RuCl}(\text{dpqMe}_2)][\text{PF}_6]$  [14]. Accordingly, there is no significant difference in the Ru–Cl bond lengths in **1** and **2** [2.387(1) and 2.391(3) Å] and reported values [12–14]. The N(1)–Ru(1)–N(2) bond angles [76.5(1) in **1**; 76.3(4)° in **2**] are similar to those of complexes  $[(\eta^6\text{-}p\text{-Pr}^i\text{C}_6\text{H}_4\text{Me})\text{RuCl}(2,3\text{-bis}(2\text{-pyridyl})\text{pyrazine})]^+$  [N(1)–Ru(1)–N(2) = 76.5(2)°] [12],  $[(\eta^6\text{-}p\text{-Pr}^i\text{C}_6\text{H}_4\text{Me})\text{RuCl}(2,3\text{-bis}(\alpha\text{-pyridyl})\text{quinoxaline})]^+$  [N(1)–Ru(1)–N(2) = 76.2(2)°] [13],  $[(\eta^6\text{-C}_6\text{H}_6)\text{RuCl}(\text{dpqMe}_2)][\text{PF}_6]$  [N(1)–Ru(1)–N(2) = 76.04(15)°] and

Table 2

Selected bond lengths (Å) and angles (°) for  $[\mathbf{1}][\text{PF}_6] \cdot (\text{C}_6\text{H}_6)_{2.5}$  and  $[\mathbf{2}][\text{PF}_6] \cdot (\text{CH}_3\text{CN})_2$

	<b>1</b> [PF <sub>6</sub> ]	<b>2</b> [PF <sub>6</sub> ]
<i>Interatomic distances</i>		
Ru1–N1	2.052(3)	2.054(10)
Ru1–N2	2.087(3)	2.091(10)
Ru1–Cl1	2.387(1)	2.391(3)
Ru1–centroid (arene)	1.681	1.684
C1–C2	1.469(5)	1.464(15)
N1–N3	1.344(4)	1.349(13)
<i>Angles</i>		
N1–Ru1–N2	76.5(1)	76.3(4)
N1–Ru1–Cl1	86.38(9)	84.4(3)
N2–Ru1–Cl1	84.79(9)	86.6(3)
Ru1–N1–C1	118.3(2)	118.7(7)
Ru1–N1–N3	121.8(2)	121.1(7)
Ru1–N2–C2	116.9(2)	116.3(7)

$[(\eta^6\text{-}p\text{-Pr}^i\text{C}_6\text{H}_4\text{Me})\text{RuCl}(\text{dpqMe}_2)][\text{PF}_6]$  [N(1)–Ru(1)–N(2) = 76.33(10)°] [14].

In the presence of benzene, compound [1][PF<sub>6</sub>] crystallises with two and a half molecules of benzene per asym-

metric unit, thus giving rise to multiple intermolecular interactions between the different components of the cell, see Fig. 5. Among these intermolecular interactions, it is noteworthy to mention the edge-to-face  $\pi$ -stacking inter-

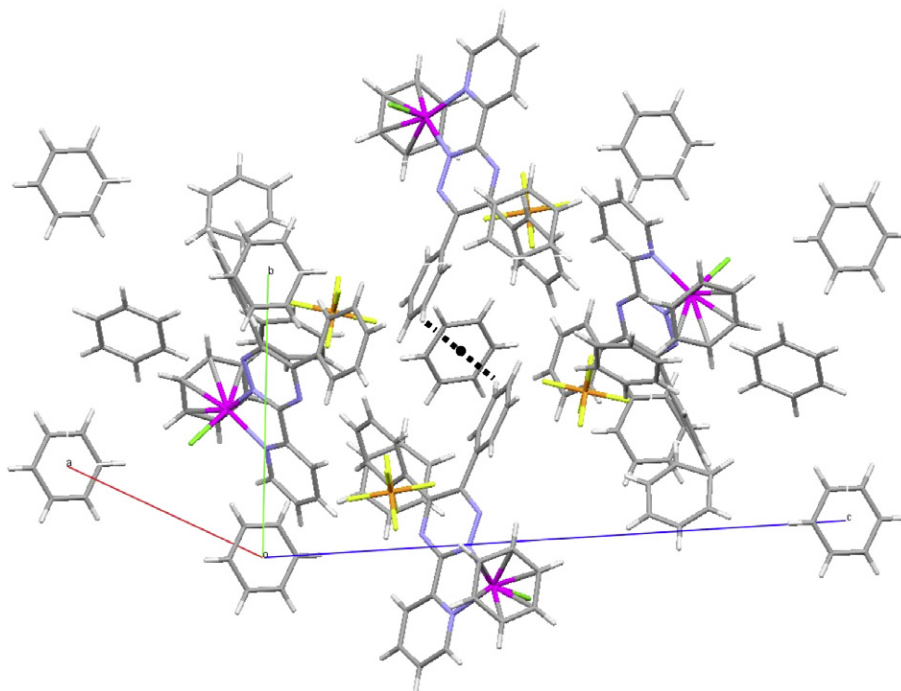


Fig. 5. Crystal packing of [1][PF<sub>6</sub>] · (C<sub>6</sub>H<sub>6</sub>)<sub>2.5</sub>.

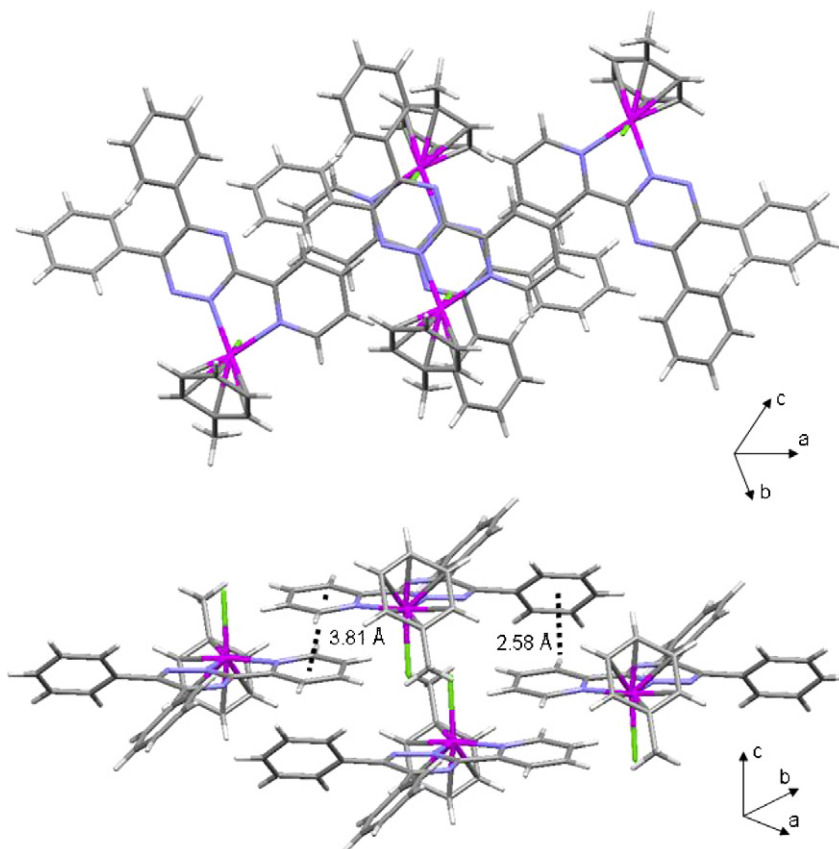


Fig. 6. Network of **2** showing the intermolecular  $\pi$ -stacking interactions.

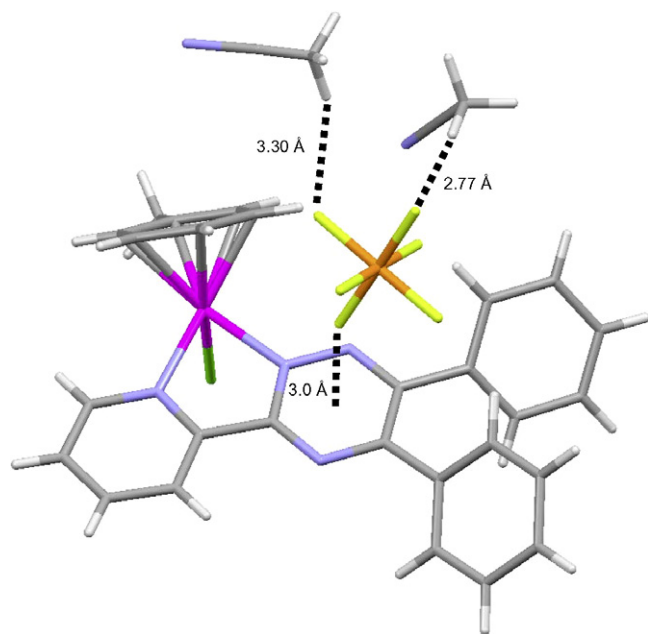


Fig. 7. Interactions involving the hexafluorophosphate anion in  $[2][PF_6] \cdot (CH_3CN)_2$ .

actions between the centrosymmetric benzene molecule and the pdpt ligand of two molecules of **1**; the C-centroid separation is 3.67 Å [H-centroid = 2.85 Å] with a C–H···centroid angle of 147.4°. Moreover, the hexafluorophosphate anion interacts with neighbouring complexes of **1** and solvent molecules through C–H···F contacts: the C···F distances ranges from 3.22 to 3.50 Å and the C–H···F angles ranging from 126.5 to 163.8°.

In the crystal packing of  $[2][PF_6] \cdot (CH_3CN)_2$ , the molecules of **2** form a network through  $\pi$ -stacking interactions between parallel aromatic rings of adjacent complexes, see Fig. 6. There are two types of  $\pi$ - $\pi$  stacking interactions involve in the multimeric system, a face-to-face and an edge-to-face types. The centroid-centroid separation of the slipped parallel interacting system (face-to-face) is 3.81 Å, while the edge-to-face C-centroid separation is 3.29 Å [H-centroid = 2.58 Å, C–H···centroid angle = 133.6°]. The distance observed between the  $\pi$ - $\pi$  interacting systems is in accordance with the theoretical value calculated for this stacking mode [15].

In addition to the  $\pi$ -stacking interactions, in the crystal packing of  $[2][PF_6] \cdot (CH_3CN)_2$ , the hexafluorophosphate anion sits on top of the cationic complex and interacts with adjacent acetonitrile molecules, see Fig. 7. The distance between the centroid of the 1,2,4-triazine ring of the pdpt ligand and the fluorine atom is 3.00 Å. The hexafluorophosphate anion interacts as well with neighbouring solvent molecules through C–H···F contacts: the C···F distances being 3.72 and 3.82 Å with C–H···F angles of 167.6 and 116.5°, respectively.

In conclusion, we have synthesised and characterised four arene ruthenium complexes with the polypyridyl che-

late ligand, 5,6-diphenyl-3-(pyridine-2-yl)-1,2,4-triazine(pdpt). As shown by the X-ray structure analysis of complexes **1** and **2**, after coordination to the ruthenium atom, the pdpt ligand possesses a free pyridyl function for intermolecular interactions. The biological activity and DNA interactions of these complexes are under investigation.

### Acknowledgements

Financial support of this work by the Swiss National Science Foundation and a generous loan of ruthenium(III) chloride hydrate from the Johnson Matthey Research Centre are gratefully acknowledged.

### Appendix A. Supplementary material

CCDC 657156 and 647515 contain the supplementary crystallographic data for  $[1][PF_6] \cdot (C_6H_6)_{2.5}$  and  $[2][PF_6] \cdot (CH_3CN)_2$ . These data can be obtained free of charge from The Cambridge Crystallographic Data Centre via [www.ccdc.cam.ac.uk/data\\_request/cif](http://www.ccdc.cam.ac.uk/data_request/cif). Supplementary data associated with this article can be found, in the online version, at [doi:10.1016/j.ica.2007.11.007](https://doi.org/10.1016/j.ica.2007.11.007).

### References

- [1] (a) M.J. Clarke, F. Zhu, D.R. Frasca, *Chem. Rev.* 99 (1999) 2511; (b) M.J. Clarke, *Coord. Chem. Rev.* 236 (2003) 209; (c) W.H. Ang, P.J. Dyson, *Eur. J. Inorg. Chem.* 20 (2006) 4003; (d) P.J. Dyson, G. Sava, *Dalton Trans.* (2006) 1929.
- [2] J.M. Rademaker-Lakhai, D. van den Bongard, D. Pluim, J.H. Beijnen, J.H.M. Schellens, *Clin. Cancer Res.* 10 (2004) 3717.
- [3] C.G. Hartinger, S. Zorbas-Seifried, M.A. Jakupec, B. Kynast, H. Zorbas, B.K. Keppler, *J. Inorg. Biochem.* 100 (2006) 891.
- [4] (a) J. Aldrich-Wright, C. Brodie, E.C. Glazer, N.W. Luedtke, L. Elson-Schwab, Y. Tor, *Chem. Commun.* (2004) 1018; (b) Y.-J. Liu, H. Chao, L.-F. Tan, Y.-X. Yuan, W. Wei, L.-N. Ji, *J. Inorg. Biochem.* 99 (2005) 530; (c) S. Schäfer, I. Ott, R. Gust, W.S. Sheldrick, *Eur. J. Inorg. Chem.* (2007) 3034; (d) A.D. Richards, A. Rodger, *Chem. Soc. Rev.* 36 (2007) 471.
- [5] (a) O. Nováková, J. Kašpárková, O. Vrána, P.M. van Vliet, J. Reedijk, V. Brabec, *Biochemistry* 34 (1995) 12369; (b) P.M. van Vliet, S.M.S. Toekimin, J.G. Haasnoot, J. Reedijk, O. Nováková, O. Vrána, V. Brabec, *Inorg. Chim. Acta* 231 (1995) 57; (c) H.-L. Chan, H.-Q. Liu, B.-C. Tzeng, Y.-S. You, S.-M. Peng, M. Yang, C.-M. Che, *Inorg. Chem.* 41 (2002) 3161; (d) P.I. Anderberg, M.M. Harding, I.J. Luck, P. Turner, *Inorg. Chem.* 41 (2002) 1365; (e) K. Karidi, A. Garoufis, A. Tsipis, N. Hadjiliadis, H. den Dulk, J. Reedijk, *Dalton Trans.* (2005) 1176.
- [6] (a) H. Chen, J.A. Parkinson, S. Parsons, R.A. Coxall, R.O. Gould, P.J. Sadler, *J. Am. Chem. Soc.* 124 (2002) 3064; (b) A. Frodl, D. Herebian, W.S. Sheldrick, *J. Chem. Soc., Dalton Trans.* (2002) 3664; (c) Y.K. Yan, M. Melchart, A. Habtemariam, P.J. Sadler, *Chem. Commun.* (2005) 4764.
- [7] (a) R.A. Zelonka, M.C. Baird, *Can. J. Chem.* 50 (1972) 3063; (b) M.A. Bennett, A.K. Smith, *J. Chem. Soc., Dalton Trans.* (1974) 233; (c) M.A. Bennett, T.-N. Huang, T.W. Matheson, A.K. Smith, *Inorg. Synth.* 21 (1982) 74.

- [8] G.M. Sheldrick, SHELXS-97 and SHELXL-97, University of Göttingen, Göttingen, Germany, 1997.
- [9] L.J. Farrugia, *J. Appl. Crystallogr.* 30 (1997) 565.
- [10] I.J. Bruno, J.C. Cole, P.R. Edgington, M. Kessler, C.F. Macrae, P. McCabe, J. Pearson, R. Taylor, *Acta Crystallogr. B* 58 (2002) 389.
- [11] (a) C.S. Araújo, M.G.B. Drew, V. Félix, L. Jack, J. Madureira, M. Newell, S. Roche, T.M. Santos, J.A. Thomas, L. Yellowlees, *Inorg. Chem.* 41 (2002) 2250;
- (b) H. Deng, J. Li, K.C. Zheng, Y. Yang, H. Chao, L.N. Ji, *Inorg. Chim. Acta* 358 (2005) 3430.
- [12] A. Singh, N. Singh, D.S. Pandey, *J. Organomet. Chem.* 642 (2002) 48.
- [13] R. Lalrempuia, M.R. Kollipara, *Polyhedron* 22 (2003) 3155.
- [14] B. Therrien, G. Süß-Fink, P. Govindaswamy, C. Saïd-Mohamed, *Polyhedron* 26 (2007) 4065.
- [15] S. Tsuzuki, K. Honda, T. Uchimura, M. Mikami, K. Tanabe, *J. Am. Chem. Soc.* 124 (2004) 104.